14th Australasian Fluid Mechanics Conference
Adelaide University, Adelaide, Australia
10-14 December 2001

Visualization of a three dimensional heaving aerofoil flow

K. D. von Ellenrieder, K. Parker and J. Soria

Laboratory for Turbulence Research in Aerospace & Combustion
Mechanical Engineering, Monash University
Clayton Campus, Victoria, 3800 AUSTRALIA

Abstract

The structure of the flow behind a three dimensional aerofoil, which performs pure heaving oscillations, is examined for a flow Reynolds number of 164, and heaving Strouhal numbers between 0.2 and 0.4. Dye flow visualization is used to study the flow from the front, side and rear of the aerofoil. A comparison with the flow around an infinite-span aerofoil with the same thickness and chord, and which operates at the same Reynolds number and Strouhal numbers, reveals that the three dimensional and two dimensional heaving aerofoil flows are substantially different. The structures in a two dimensional foil flow are predominantly orientated along the spanwise direction. In contrast, v-shaped vortex structures, which are partially aligned with the aerofoil wingtips, are formed in a finite-span aerofoil flow.

Introduction

Recent experimental work on the flow around two dimensional pitching and heaving (plunging) aerofoils has demonstrated that it is possible to generate thrust with an efficiency of almost 87% [1],[2]. When thrust is produced in this manner, the average velocity profile of the flow behind the aerofoil has the form of a jet [8] and is characterized by a train of vortices [4],[6], which has been descriptively called a "reverse von Karman vortex street". The creation of this average jet-like flow has been found to occur over a large range of Reynolds numbers $1100 \leq Re \leq 40000$ and for Strouhal numbers of $0.25 \leq St \leq 0.35$ [8]. The structure of the flow behind the aerofoil is strongly dependent upon the Strouhal number and phase angle (ψ) between heave and pitch motions, and is affected by vortex shedding from both the leading- and trailing-edge of the aerofoil. As mentioned in [1] and [7], the effects of the Reynolds number is believed to be of secondary importance.

When an finite-span oscillating aerofoil is used to produce thrust in nature or engineering applications the flow created by the foil motion will be three dimensional. The flow behind a two dimensional foil will only contain span-wise vortices, whereas the motion of a three dimensional foil will also produce stream-wise (wingtip) vortices. Thus, not only is the structure of the flow different, but the efficiency determined using two dimensional theory and experiments may be overestimated because not all of the wake energy losses are considered [3].

The work presented in this paper is the result of a preliminary investigation — it is part of a larger research program to characterize the effects of phase angle, Strouhal number, and pitch amplitude on the thrust, power efficiency, and flow around three dimensional oscillating foils. The intent of this investigation is to gain a qualitative understanding of the nature of the three dimensional flow as a guide for the design of the experimental apparatus to be used in the full study. Here we focus only on the fluid mechanics and present the results of a series of experiments performed on the flow around both a three dimensional "finite-span" aerofoil and a two dimensional "infinite-span" aerofoil. The aerofoils have a constant pitch angle of 0° and undergo a sinusoidal heaving motion in the vertical direction. The Reynolds number (based on freestream velocity, aerofoil chord length, and kinematic viscosity) is $Re = 164$ and flow images were made at Strouhal numbers (based on heave frequency, freestream velocity, and the double-amplitude of the heaving oscillation) of $St = \{0.20, 0.25, 0.30, 0.35, 0.40\}$. As shown in figure 1, fluorescent dye flow images were recorded from three different vantage points.

Experimental Apparatus and Methods

A re-circulating water tunnel, which has a test section of 100 mm × 100 mm and is 800 mm long, was used to conduct the experiments. The contraction, which is located between the settling chamber and test section, has a 9 : 1 area ratio. The average velocity of the flow in the test section can be continuously varied from 5 mm/s to 115 mm/s using a gate valve and flow rate meter.

The aerofoils, which have a symmetrical cross-section and rectangular planform, are constructed from streamlined sections of aluminium model aeroplane strut tubing. Both of the foils are hollow, have a chord length (c) of 19.2 mm and a thickness (t) of $t/c = 0.3$. The aspect ratio of the three dimensional foil is $AR = 2.1$ ($AR = b/c$, where b is the aerofoil span). The two dimensional foil is 90 mm long in the spanwise direction and is mounted between perspex endplates; these endplates are attached to a boom, which is located outside the test section. A line of dye injection holes, which have a diameter of 0.9 mm and are positioned at 2.0 mm intervals, lies along the leading-edge of each aerofoil. A brass tube (90 mm long with a 2.4 mm outer diameter) is press-fit and glued into the centre of the top surface of the finite span aerofoil. This tube serves as both the aerofoil sting and as part of the dye injection system. Dye is fed into the two dimensional foil through each endplate.

The heaving motion of the aerofoils is produced by attaching the aerofoil assemblies to a lead-screw-driven, linear translation stage (figure 2). The translation stage is vertically mounted above the test section and is oscillated using a computer-controlled stepper motor. A cosine motion profile is used and the oscillation frequency is checked by measuring the limit/home switch feedback signal from the translation stage with an oscilloscope. The double-amplitude of the motion was kept constant at 19.2 mm ($A_{te}/c = 1.0$, where A_{te} is the trailing-edge displacement) and the average freestream velocity was fixed at 8.5 mm/s; the Strouhal number was then varied by changing the oscillation frequency of the translation stage.

In order to visualize the flow, laser light is used to illuminate Kiton Red 620 fluorescent dye. The dye is fed from a bottle, which is mounted approximately 1.0 m above the test section. The dye flow rate was controlled using a small needle valve. A 6 mm diameter cylindrical lens is used to expand the beam from a 200 mW, Nd:YVO_4, diode laser (532 nm wavelength) into a light sheet. A second cylindrical lens (-19 mm focal length) could be

placed in the light sheet to illuminate a volume of the flow. Images of the flow are captured with a CCD video camera and VCR tape recorder.

Results & Discussion

Figure 3 shows a pair of images taken from view 2 (see figure 1) with a vertical light sheet, which is orientated parallel to the flow. In the case of the two dimensional aerofoil flow the streaklines illuminated by the dye reveal a regular, mushroom-shaped vortex structure, which convects downstream (figure 3*a*). Structures similar to this are present in the lower-amplitude ($A_{te}/c = 0.4$; $St = 0.48$) heaving aerofoil study of [5] and also in the pure-pitching aerofoil work of [6]. In contrast, the structures exposed by a light sheet in the three dimensional aerofoil flow (figure 3*b*) are complex and irregular. Here, owing to the out-of-plane velocity components present in the flow, the vortex structures move in and out of view as they convect downstream.

The substantial differences between the flows around the two dimensional and the three dimensional aerofoil can be seen in figure 4. The image is taken from view 3 and a three dimensional region of the flow has been illuminated. In the two dimensional aerofoil case (figure 4*a*) the flow is uniform across the span of the foil and the s-shaped streaklines revealed by the dye remain nearly parallel as they convect downstream. On the other hand, the flow around the finite-span aerofoil is quite three dimensional. In figure 4*b* it can be seen that the streaklines seem to have rolled-up into vortex tubes that lie nearly parallel to the path traced by the aerofoil wingtip. Structures that are initially spanwise are stretched in the downstream direction along the centre-line of the foil, but remain attached to the wingtips to form a v-shaped structure.

This v-shaped vortex structure is more clearly visible in figures 5(*a*–*i*). The sequence of images, which are arranged from left to right then top to bottom, illustrate the evolution of the vortex structures behind a three dimensional aerofoil during one heave cycle. In figure 5*a* a v-shaped structure, which formed in the preceeding heave cycle, can be seen in the centre of the picture. The aerofoil is located at the lower extreme of the heave displacement and has started to move upwards. Immediately behind the aerofoil a vortex structure is present and in figures 5(*a*–*e*) it begins to catch up to the first v-shaped vortex structure. As it convects, this vortex structure is stretched in the downstream direction along the aerofoil centreline, but remains attached to the wingtips. In figure 5*e* a third vortex structure can be seen forming behind the aerofoil. This third structure forms a sharp v-shaped structure similar to the one located in the centre of figure 5*a*. Thus, during each heave cycle two vortex structures are formed, one at the top of the cycle (top vortex) and one at the bottom of the cycle (bottom vortex). The top vortex always forms a sharper v-shaped structure. The most likely reason for this is the presence of the sting, which is located on the upper surface of the aerofoil. The top vortex originates from fluid which passes underneath the aerofoil. This vortex is probably stronger than the bottom vortex, which consists of fluid that has passed around the sting or in the wake of the sting. Thus, the stronger self-induced motion of the top vortex creates a more pronounced v-shaped structure.

Lastly, the dependence of the wake structure on Strouhal number can be seen in figure 6. As the Strouhal number is decreased the streamwise wavelength of the vortex structures behind the aerofoil decreases. In each of the images the aerofoil is located at the lower extremity of the heave displacement. However, the v-shaped structure visible in figures 5(*a*–*b*) is modified. In the higher Strouhal number cases, the v-shaped vortex structure doesn't become pronounced until after the aerofoil has begun to move upwards — a phase lag seems to occur. Additionally, the core size of the v-shaped structures decreases with increasing St.

Concluding Remarks

The form of the flow behind a finite-span heaving aerofoil is substantially different from that produced by a two dimensional aerofoil with the same thickness and chord, and which is operating at the same Reynolds number and Strouhal number. The vortex structures trailing a two dimensional aerofoil are aligned in the spanwise direction for many chordlengths behind the aerofoil. In a three dimensional aerofoil flow the wingtip vortices are connected to a significantly smaller spanwise vortex section, and form a structure with an overall v-shape. Thus, as predicted by [3], one would expect the thrust generation efficiency of a finite-span aerofoil to be different from that of a two dimensional aerofoil.

Additionally, we have found that the sting affects the shape of the vortex structures created by the three dimensional heaving aerofoil. Here, the ratio of the sting diameter to the aerofoil span is 6%, yet the vortex structure which is produced at the bottom of the heave cycle seems to be much weaker than the vortex structure that is produced at the top of the cycle. It will be necessary to take this into consideration in the future pitching aerofoil experiments we have planned: a bearing will be mounted in the centre of the aerofoil, which will allow it to pitch. This result also suggests that in a natural heaving foil flow, such as might occur behind a fish, the body to which the foil is attached can have a significant influence on the structure of the flow.

References

[1] Anderson, J.M., Streitlien, K., Barrett, D.S., and Triantafyllou, M.S., Oscillating foils of high propulsive efficiency, *J. Fluid Mech.*, **360**, 1998, 41–72.

[2] Barrett, D.S., Triantafyllou, M.S., Yue, D.K.P., Grosenbaugh, M.A., and Wolfgang, M.J., Drag reduction in fish-like locomotion, *J. Fluid Mech.*, **392**, 1999, 183–212.

[3] Cheng, H.K. and Murillo, L.E. Lunate-tail swimming propulsion of curved lifting-line in unsteady flow. Part 1. Asymptotic Theory, *J. Fluid Mech.*, **143**, 1984, 327–350.

[4] Freymuth, P., Propulsive vortical signature of plunging and pitching airfoils, *AIAA J.*, **26:7**, 1988, 881–883.

[5] Jones, K.D., Dohring, C.M., and Platzer, M.F., Experimental and computational investigation of the Knoller-Betz effect, *AIAA J.*, **36:7**, 1988, 1240–1246.

[6] Koochesfahani, M.M., Vortical patterns in the wake of an oscillating airfoil, *AIAA J.*, **27:9**, 1989, 1200–1205.

[7] Ohmi, K., Coutanceau, M., Loc, T.P., and Dulieu, A., Vortex formation around an oscillating and translating airfoil at large incidences, *J. Fluid Mech.*, **211**, 1990, 37–60.

[8] Triantafyllou, G.S., Triantafyllou, M.S., and Grosenbaugh, M.A., Optimal thrust development in oscillating foils with application to fish propulsion, *J. Fluid Struct.*, **7**, 1993, 205–224.

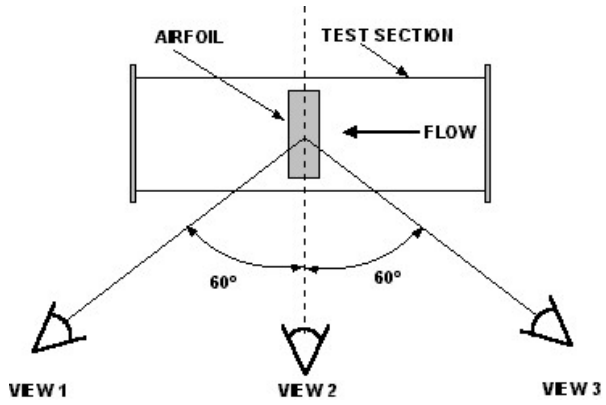

Figure 1: Plan view of the test section; the three vantage points used to film the flow are indicated with a small "eye".

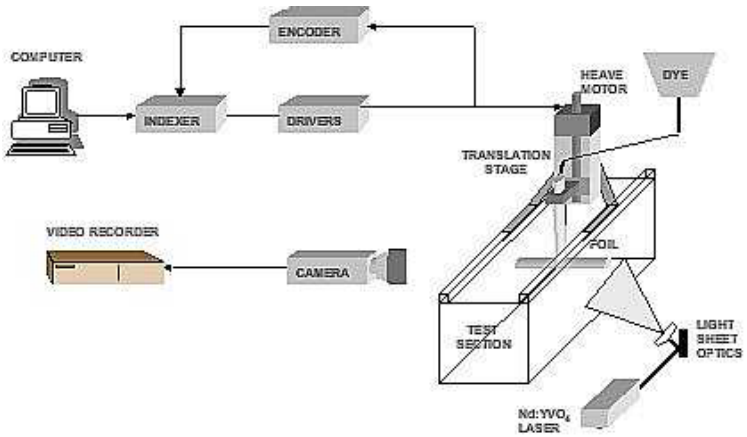

Figure 2: Experimental setup.

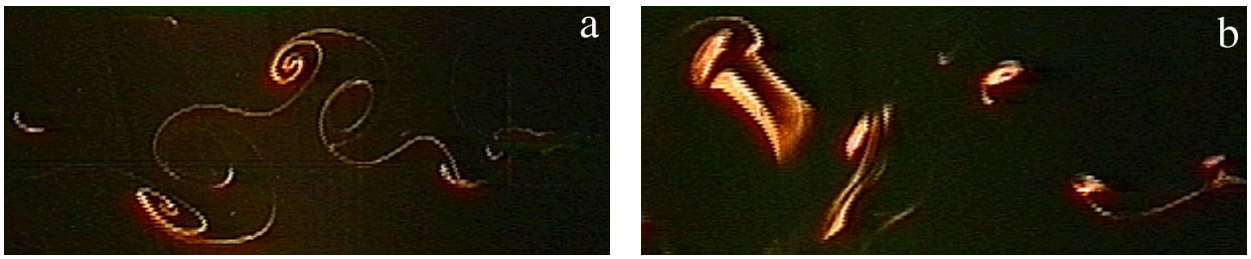

Figure 3: A two dimensional slice of the flow behind the infinite span aerofoil (a) and the finite span aerofoil (b). The images were made from view 2 using a thin light sheet. For both images $St = 0.3$ and $Re = 164$.

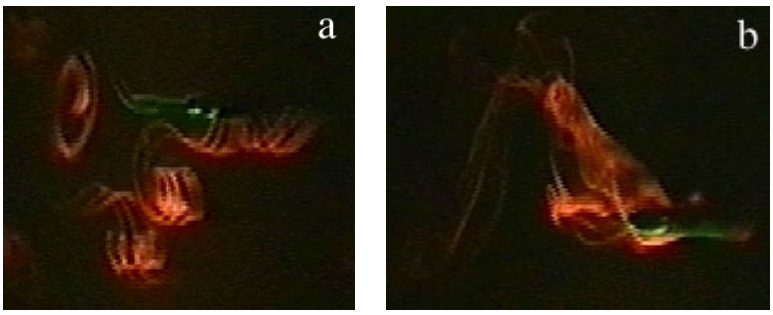

Figure 4: Vortex structures in the flow behind the infinite span aerofoil (a) and the finite span aerofoil (b). The images were made from view 3 and a volume of the flow is illuminated. For both images $St = 0.35$ and $Re = 164$.

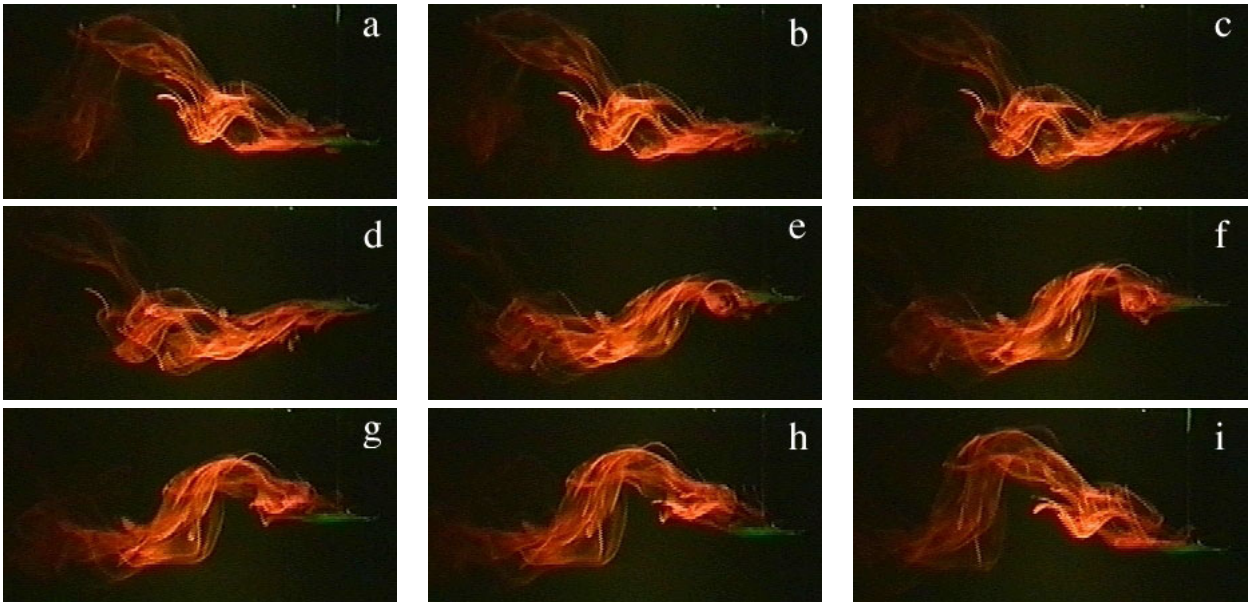

Figure 5: Evolution of the vortex structures in the flow behind the finite span aerofoil during one heave cycle. The images were made from view 1 and a volume of the flow is illuminated. Here $St = 0.25$ and $Re = 164$.

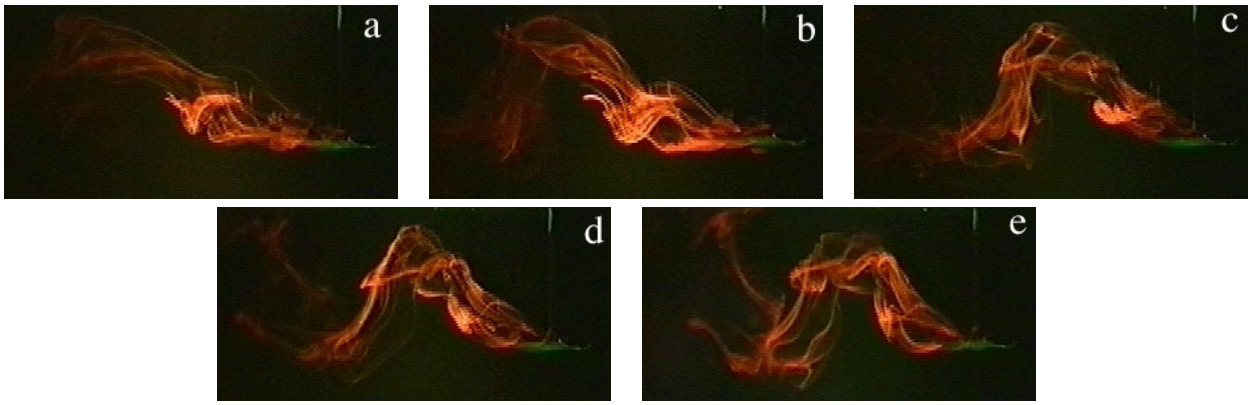

Figure 6: Strouhal number dependence of the structures in the flow behind the finite span aerofoil. The images were made from view 1 and a volume of the flow is illuminated. The Strouhal number is (a) 0.20, (b) 0.25, (c) 0.30, (d) 0.35, (e) 0.40 and in all images $Re = 164$.